Journal of Power Sources 222 (2013) 426–441

Contents lists available at SciVerse ScienceDirect

Journal of Power Sources

journal homepage: www.elsevier.com/locate/jpowsour

Reduced order model for a lithium ion cell with uniform reaction rate approximation

V. Senthil Kumar*

India Science Lab, General Motors Global R & D, Creator Building, International Technology Park, Whitefield Road, Bangalore 560066, India

HIGHLIGHTS

- ► Physics based reduced order model for lithium ion cells.
- ► Model reduction based on volume averaging and profile based approximations.
- ► Amenable for battery management system algorithms, detailed parameter estimation etc.

ARTICLE INFO

Article history:
Received 16 June 2012
Received in revised form
3 September 2012
Accepted 5 September 2012
Available online 10 September 2012

Keywords:
Lithium ion cell
Reduced order model
Battery management system
Volume averaging
Profile based approximations

ABSTRACT

The detailed isothermal electrochemical model for a lithium ion cell comprises of 10 coupled partial differential equations (PDEs). It is computationally intensive to use this model for detailed parameter estimation, battery packs, battery management system algorithms, calendar or cycle life predictions etc. This work describes a reduced order model framework, which reduces the detailed model PDEs, to a manageable set of ordinary differential equations (ODEs), which can be used for the above applications. Volume averaging PDEs yield ODEs. Hence volume averaging is the basic method used for model reduction. The gradient or profile information lost on volume averaging is recovered through profile based approximations. For the lowest order reduced order model (ROM), a uniform reaction rate, quadratic electrolyte concentrations and quartic solid phase concentrations are assumed. In this ROM only 5 linear ODEs are solved, and the rest are nonlinear algebraic evaluations. When compared with the detailed electrochemical model of a lithium ion cell, this ROM gives negligible error at nominal currents and a maximum error of about 3% at high currents, for a typical commercial cell.

1. Introduction

Consider a lithium ion cell discharging current through a load, as in Fig. 1. Say the negative electrode is graphite. When the cell is in charged state lithium exists as the lithium carbide (LiC_6) in the negative electrode. During discharge LiC_6 breaks down releasing Li^+ ions into the electrolyte, and the electrons to the collector (through the solid conducting matrix of the negative electrode particles), which eventually flow into the external circuit. The electrons travel from the negative electrode to the positive electrode through the external circuit, while the Li^+ ions travel in the electrolyte from the negative electrode to the positive electrode. Say the positive electrode is some lithium metal oxide. The electrons (flowing through the external circuit) and Li^+ ions (diffusing through the electrolyte) combine on the surface of the positive electrode particles to form neutral Li species, which then intercalate into lithium metal oxide. The intercalation reactions occurring during the discharge are reversible and the reverse reactions occur during charge.

Electrodes contain a solid phase comprising of active materials (and other additives), and a liquid electrolyte phase. Separator typically has some solid polymeric membrane and a liquid electrolyte phase. Neglecting the solid additives and inert polymeric membranes, there are totally five phases: active materials in the two electrodes and electrolyte phase in the three regions. For an isothermal operation of a single cell, drawing the mass and charge balances for these five phases, the detailed electrochemical model comprises of ten coupled partial differential equations (PDEs), Refs. [1,2]. It is computationally intensive (or often impossible) to use this detailed electrochemical model for

- *Battery packs*, since they have hundreds of single cells in series – parallel configurations.
- *Battery management system algorithms*, since on-board computational capabilities are nominal. Currently electrical

* Present address: Samsung Advanced Institute of Technology – India, SISO Private Ltd., Bangalore 560 093, India. Tel.: +91 80 4181 9999; fax: +91 80 4181 9000.
E-mail address: senthil.v.kumar@gmail.com.

0378-7753/$ – see front matter © 2012 Elsevier B.V. All rights reserved.
http://dx.doi.org/10.1016/j.jpowsour.2012.09.013

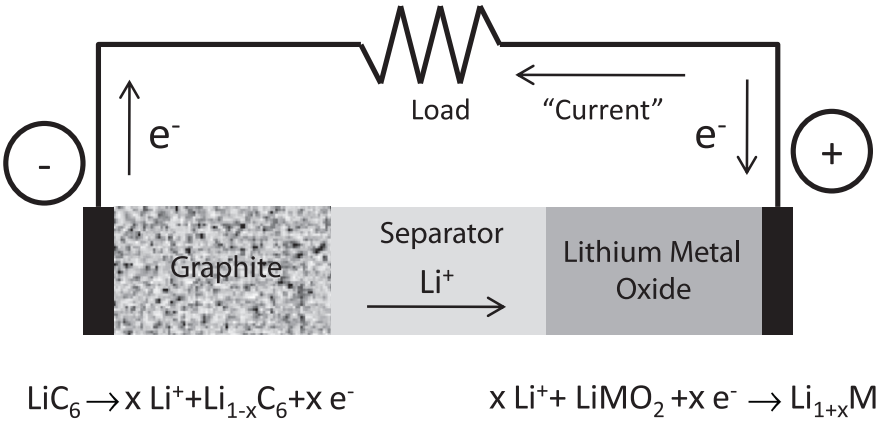

Fig. 1. Discharge of a lithium ion cell.

circuit based models are used for battery management systems, due to their minimal mathematical complexity (first order ordinary differential equations based mathematical structure).
- *Calendar or cycle life predictions*, since the model needs to predict cell behavior for real time periods as long as a few months.
- *Detailed parameters estimation*, since systematic optimization of parameters embedded within ten coupled PDEs is formidable.
- *inclusion of complex degradation mechanisms*, since they add to the numerical stiffness.

The aim of this work is to develop a reduced order model framework, which reduces the detailed electrochemical model comprising of ten PDEs for the isothermal behavior of a single cell, to a manageable set of ordinary differential equations (ODEs), which can be used for the above applications. It is preferred that the reduced order model framework has the following mathematical properties:

- It has minimal computational requirements so that it can be implemented in on-board battery management systems. It is numerically stable and easily optimized during parameter estimations. These properties are ensured if the model equations are first order ODEs (linear or nonlinear, could be coupled). Volume averaging PDEs yield ODEs. Hence volume averaging is the basic methodology used in this work for physics based model reduction.
- The model predictions should be grid or system size independent. For example, one could discretize the governing PDEs, with say 10 or 20 nodes for each electrode or separator region, as in the Method of lines. Model predictions in such a scenario will often be grid size dependent, and will give higher errors if the electrode or separator regions get thicker. Thus, ODEs should be solved not for the discretized original PDEs, but for physically relevant internal variables, which parameterize the internal field profiles. For example, in profile based approximations, interfacial concentrations are solved, and the concentration profiles in the individual regions are expressed in terms of these interfacial concentrations. A brief literature review of profile based approximations is given below.
- It has systematic mathematical approximations rather than phenomenological approximations. For example, a single particle model Ref. [3] neglects electrolyte potential and electrolyte concentration variations. Hence, a single particle model cannot work at high currents. If a reduced order model is, however, based on systematic mathematical approximations, relaxing those approximations one can derive higher order models, which work at all scenarios. For example, the current work approximates the local reaction rates in an electrode to be the volume average reaction rates. This approximation can be relaxed to allow spatial variation of reaction rates, will be reported in future.

Solution of partial differential equations through profile based approximations was developed by Pohlhausen (1921) for a problem in laminar boundary layer theory, Ref. [4, p. 41]. He used a quartic velocity profile to satisfy the momentum integral equation and the relevant boundary conditions. Glueckauf (1955) [5] used a parabolic concentration profile to describe the diffusion in a sphere, in the context of chromatography. Ref. [6] used the parabolic approximation for diffusion in a sphere to describe the kinetics of adsorption in a fixed bed of spheres. Refs. [7,8], for example, describe higher order polynomial approximations for diffusion in a sphere. Ref. [9] extended these methods to reaction and diffusion in spherical and slab geometries. Ref. [10] reports parabolic and quartic profile based approximations for diffusion in active material spheres in the electrodes of a lithium ion cell. This work extends the profile based approximation for the rectangular electrolyte concentration fields in electrode and separator regions as well.

Sections 2–5 present the detailed field equations and derive the reduced order equations for solid phase current balances, electrolyte phase mass balances, total current balances and solid phase mass balances, respectively. These equations are the core conservation equations governing the isothermal behavior of a single cell. The results from these sections feed into the Butler–Volmer kinetics, in Section 6, for the electrochemical reactions happening on the surface of the active material spheres in the electrode regions. The reduced order model is derived across Sections 2–6. Often the derivation sequence is different from the computational sequence. Hence, the reduced order model results are collated in an algorithmic order in Section 7. The cell voltage predictions by the reduced order model are compared with those from the detailed electrochemical model for constant current and pulse protocols in Section 8.

2. Solid phase current balance equations

2.1. Field equations

Ohm's law is typically written for a one-dimensional conductor as $I = V/R$, where I is the current in Amperes (A), V the voltage in

Volts (V) and R the resistance in Ohms (Ω). It is generalized to a three-dimensional continuum as $I = E/\rho$, where I is the current density in A m^{-2}, E is the electric field in V/m, and ρ the resistivity in Ωm. Conductivity, σ, is the reciprocal of resistivity, with units Siemens m^{-1}, where 1 Siemens = 1 Ω^{-1}. Thus, Ohm's law for a continuum is $I = -\sigma\nabla\Phi$. Ohm's law describes the relationship between current density and potential field in a conductor. In the cell electrodes, the electrochemical reactions generate or consume electrons. Hence, the gradient of current density within the electrodes is proportional to electrochemical reaction rate. These equations are the solid phase current balance equations in the two electrodes, given below along with their boundary conditions. At the two collector ends, solid current density equals the total current density, computed as external current per unit electrode cross sectional area. At the separator interfaces, solid current is zero, so that within the separator the current is fully ionic.

2.1.1. Negative electrode region

$$\frac{\partial}{\partial x}\left(-\sigma_{1n}\frac{\partial\Phi_1}{\partial x}\right) = -a_n F j_n, \tag{1}$$

$$\text{Boundary conditions :} \quad -\sigma_{1n}\frac{\partial\Phi_1}{\partial x}\bigg|_{x=0} = I, \text{ and} \tag{2}$$

$$-\sigma_{1n}\frac{\partial\Phi_1}{\partial x}\bigg|_{x=l_n} = 0. \tag{3}$$

2.1.2. Positive electrode region

$$\frac{\partial}{\partial x}\left(-\sigma_{1p}\frac{\partial\Phi_1}{\partial x}\right) = -a_p F j_p, \tag{4}$$

$$\text{Boundary condition :} \quad -\sigma_{1p}\frac{\partial\Phi_1}{\partial x}\bigg|_{x=l_n+l_s} = 0, \text{ and} \tag{5}$$

$$-\sigma_{1p}\frac{\partial\Phi_1}{\partial x}\bigg|_{x=L} = I. \tag{6}$$

2.2. Volume averaged field equations

Volume average of a function $f(x,t)$ in the electrode regions is defined as follows:

$$\langle f\rangle_n(t) = \frac{1}{Al_n}\int_{x=0}^{l_n} f(x,t)A\,dx = \frac{1}{l_n}\int_{x=0}^{l_n} f(x,t)dx, \tag{7}$$

$$\langle f\rangle_p(t) = \frac{1}{Al_p}\int_{x=l_n+l_s}^{L} f(x,t)A\,dx = \frac{1}{l_p}\int_{x=l_n+l_s}^{L} f(x,t)dx. \tag{8}$$

For example the volume average reaction rate in the negative electrode is

$$\langle j_n\rangle(t) = \frac{1}{l_n}\int_{x=0}^{l_n} j_n(x,t)dx. \tag{9}$$

A field equation is volume averaged by integrating it over its domain, and normalizing with the domain volume. For example, equation (1) is integrated as follows:

$$\frac{1}{l_n}\int_{x=0}^{l_n} d\left(-\sigma_{1n}\frac{\partial\Phi_1}{\partial x}\right) = -a_n F\frac{1}{l_n}\int_{x=0}^{l_n} j_n\,dx \Rightarrow \frac{1}{l_n}\left(-\sigma_{1n}\frac{\partial\Phi_1}{\partial x}\right)_{x=0}^{l_n} = -a_n F\langle j_n\rangle. \tag{10}$$

Applying the boundary conditions (2) and (3) as the lower and upper limits of integration in equation (10) give

$$I = a_n l_n F\langle j_n\rangle. \tag{11}$$

Similarly volume averaging equation (4) gives

$$I = -a_p l_p F\left\langle j_p\right\rangle. \tag{12}$$

Equating equations (11) and (12) and rearranging gives

$$a_n l_n\langle j_n\rangle(t) + a_p l_p\left\langle j_p\right\rangle(t) = 0. \tag{13}$$

In a closed circuit, the electrons generated in an electrode are consumed in the other electrode, with no loss of electrons in the external circuit. Equation (13) accounts for this overall electroneutrality.

Equations (11) and (12) can be rearranged to get an expression for the average reactions rates in the electrodes as

$$\langle j_n\rangle(t) = \frac{I(t)}{a_n F l_n}, \text{ and} \tag{14}$$

$$\left\langle j_p\right\rangle(t) = -\frac{I(t)}{a_p F l_p}. \tag{15}$$

Equations (14) and (15) relate the volume average reaction rates in the electrodes to the external current, at any time. These results are exact, since volume averaging is an exact operation and not an approximation. Of course, a volume averaged field equation has lost information about the profile or gradient of a quantity. The profile or gradient information will be recovered from the field equation by profile approximation, as shown below.

For a constant current discharge, the volume average reaction rates in the electrodes, equations (14) and (15), are constant. If by convention, discharge current has a positive sign, then the volume average reaction rate in the negative electrode is positive, while that in the positive electrode is negative. These signs are consistent with the fact that during discharge Li^+ ions are released in the negative electrode region and consumed in the positive electrode region.

2.3. Profile approximations

In the *uniform reaction rate approximation*, the local reaction rate is assumed to be the volume average reaction rate, at any time i.e.

$$j_n(x,t) \approx \langle j_n\rangle(t) = \frac{I(t)}{a_n F l_n}, \text{and} \tag{16}$$

$$j_p(x,t) \approx \left\langle j_p\right\rangle(t) = -\frac{I(t)}{a_p F l_p}. \tag{17}$$

The errors in these approximations vanish at the volume averaged level.

Any spatio-temporal quantity can be written as a sum of its time varying volume average and a spatio-temporal deviation term, for

example the negative electrode reaction rate can always be written as

$$j_n(x,t) = \langle j_n\rangle(t) + j_n^d(x,t). \quad (18)$$

In the leading order uniform reaction rate approximation, the deviation term is neglected. This work explores the limits of applicability of the leading order volume average reaction rate term.

With the uniform reaction rate approximation, the negative electrode solid current balance (1) becomes

$$\frac{\partial}{\partial x}\left(-\sigma_{1n}\frac{\partial \Phi_1}{\partial x}\right) \approx -a_n F\langle j_n\rangle(t) = -\frac{I(t)}{l_n}. \quad (19)$$

The above equation is integrated with respect to x to get

$$-\sigma_{1n}\frac{\partial \Phi_1}{\partial x} = -\frac{I(t)}{l_n}x + f(t), \quad (20)$$

where $f(t)$ is some arbitrary function. Using the boundary condition (3) gives

$$0 = -\frac{I(t)}{l_n}l_n + f(t). \quad (21)$$

Eliminating $f(t)$ in equation (20) using equation (21) gives the solid current in negative electrode, under uniform reaction rate approximation, as

$$-\sigma_{1n}\frac{\partial \Phi_1}{\partial x} = \frac{I(t)}{l_n}(l_n - x). \quad (22)$$

Note that equation (22) satisfies the other boundary condition (2). Similarly the solid current in the positive electrode, under uniform reaction approximation is

$$-\sigma_{1p}\frac{\partial \Phi_1}{\partial x} = \frac{I(t)}{l_p}[x - (l_n + l_s)]. \quad (23)$$

Thus uniform reaction rate approximation implies a linear solid current profile in the electrodes i.e. the solid current density linearly varies from the total current density at the collector end to zero at the separator end. Hence, a test of the solid current linearity is a test of uniform reaction rate approximation; the numerical results are presented in supplementary material S1.

3. Electrolyte phase mass balance equations

Ref. [10] reports profile based approximations for diffusion in spherical active material particles in the electrodes. This work extends that approach for the rectangular electrolyte concentration fields in the electrode and separator regions.

3.1. Field equations

The electrolyte diffusion equations form the electrolyte phase mass balances. The reaction rate terms (described in the previous section) form source or sink terms in the electrode regions, while electrolyte accumulates and diffuses through the separator. Electrolyte concentration field is continuous through the three regions: negative electrode, separator and positive electrode. Hence, the concentration and flux continuities hold at the electrode–separator interfaces. The interfacial concentrations (c_{2in},c_{2ip}) and fluxes (q_{2in},q_{2ip}) are identified as separate variables, so that it is easy to impose them in the individual regions, and maintain their equality across interfaces. At the collector ends zero flux boundary conditions apply.

3.1.1. Negative electrode region

$$\varepsilon_{2n}\frac{\partial c_2}{\partial t} = \frac{\partial}{\partial x}\left(D_{2n}\frac{\partial c_2}{\partial x}\right) + a_n(1-t_+)j_n, \quad (24)$$

with boundary conditions

$$-D_{2n}\frac{\partial c_2}{\partial x}\Big|_{x=0} = 0, \quad (25)$$

$$c_2(l_n,t) = c_{2in}, \quad (26)$$

$$-D_{2n}\frac{\partial c_2}{\partial x}\Big|_{x=l_n} = q_{2in}. \quad (27)$$

3.1.2. Separator region

$$\varepsilon_{2s}\frac{\partial c_2}{\partial t} = \frac{\partial}{\partial x}\left(D_{2s}\frac{\partial c_2}{\partial x}\right), \quad (28)$$

with boundary conditions

$$c_2(l_n,t) = c_{2in}, \quad (29)$$

$$-D_{2s}\frac{\partial c_2}{\partial x}\Big|_{x=l_n} = q_{2in}, \quad (30)$$

$$c_2(l_n+l_s,t) = c_{2ip}, \quad (31)$$

$$\text{and } -D_{2s}\frac{\partial c_2}{\partial x}\Big|_{x=l_n+l_s} = q_{2ip}. \quad (32)$$

3.1.3. Positive electrode region

$$\varepsilon_{2p}\frac{\partial c_2}{\partial t} = \frac{\partial}{\partial x}\left(D_{2p}\frac{\partial c_2}{\partial x}\right) + a_p(1-t_+)j_p, \quad (33)$$

with boundary conditions

$$c_2(l_n+l_s,t) = c_{2ip}, \quad (34)$$

$$-D_{2p}\frac{\partial c_2}{\partial x}\Big|_{x=l_n+l_s} = q_{2ip}, \quad (35)$$

$$\text{and } -D_{2p}\frac{\partial c_2}{\partial x}\Big|_{x=L} = 0. \quad (36)$$

Across the three regions, the initial condition is

$$c_2(x,0) = c_{20}. \quad (37)$$

3.2. Volume averaged field equations

The volume average definitions for a function $f(x,t)$ in the negative and positive electrode regions are as defined earlier in equations (7) and (8). The corresponding definition in the separator region is

$$\langle f\rangle_s(t) = \frac{1}{Al_s}\int_{x=l_n}^{l_n+l_s} f(x,t)A\,dx = \frac{1}{l_s}\int_{x=l_n}^{l_n+l_s} f(x,t)dx. \tag{38}$$

The electrolyte diffusion equation in the negative electrode region, equation (24) is volume averaged as follows:

$$\frac{1}{l_n}\int_{x=0}^{l_n}\left[\varepsilon_{2n}\frac{\partial c_2}{\partial t} = \frac{\partial}{\partial x}\left(D_{2n}\frac{\partial c_2}{\partial x}\right) + a_n(1-t_+)j_n\right]dx. \tag{39}$$

In the left hand side of equation (39), the volume average of the time derivative becomes the time derivative of the volume average

$$\text{LHS} = \frac{\varepsilon_{2n}}{l_n}\int_{x=0}^{l_n}\frac{\partial c_2}{\partial t}dx = \varepsilon_{2n}\frac{d}{dt}\left(\frac{1}{l_n}\int_{x=0}^{l_n} c_2\,dx\right) = \varepsilon_{2n}\frac{d\langle c_2\rangle_n}{dt}. \tag{40}$$

The diffusive flux gradient term in the right hand side of equation (39) gets volume averaged, using the boundary conditions (25) and (27) as follows:

$$\left\langle\frac{\partial}{\partial x}\left(D_{2n}\frac{\partial c_2}{\partial x}\right)\right\rangle_n = \frac{1}{l_n}\int_{x=0}^{l_n}\frac{\partial}{\partial x}\left(D_{2n}\frac{\partial c_2}{\partial x}\right)dx = \frac{1}{l_n}\left(D_{2n}\frac{\partial c_2}{\partial x}\right)_{x=0}^{l_n} = -\frac{q_{2in}}{l_n}. \tag{41}$$

The volume average of the reaction rate term in the right hand side of equation (39) is straight forward:

$$\langle a_n(1-t_+)j_n\rangle_n = \frac{1}{l_n}\int_{x=0}^{l_n} a_n(1-t_+)j_n\,dx = a_n(1-t_+)\langle j_n\rangle. \tag{42}$$

Putting together the results from equations (40)–(42), and multiplying by the electrode thickness, the volume averaged electrolyte diffusion equation in the negative electrode region is

$$l_n\varepsilon_{2n}\frac{d\langle c_2\rangle_n}{dt} = -q_{2in} + (1-t_+)a_n l_n\langle j_n\rangle. \tag{43}$$

In the separator region, the diffusive flux gradient term in the right hand side of equation (28) gets volume averaged, using the boundary conditions (30) and (32) as follows:

$$\left\langle\frac{\partial}{\partial x}\left(D_{2s}\frac{\partial c_2}{\partial x}\right)\right\rangle_s = \frac{1}{l_s}\int_{x=l_n}^{l_n+l_s}\frac{\partial}{\partial x}\left(D_{2s}\frac{\partial c_2}{\partial x}\right)dx = \frac{1}{l_s}\left(D_{2s}\frac{\partial c_2}{\partial x}\right)_{x=l_n}^{l_n+l_s} = \frac{q_{2in}}{l_s} - \frac{q_{2ip}}{l_s}. \tag{44}$$

Volume averaging of the accumulation term in equation (28) is as before. Finally, the volume averaged electrolyte diffusion equation in the separator region is

$$l_s\varepsilon_{2s}\frac{d\langle c_2\rangle_s}{dt} = q_{2in} - q_{2ip}. \tag{45}$$

In the positive electrode region, the diffusive flux term in the right hand side of equation (33) gets volume averaged, using the boundary conditions (35) and (36) as follows:

$$\left\langle\frac{\partial}{\partial x}\left(D_{2p}\frac{\partial c_2}{\partial x}\right)\right\rangle_p = \frac{1}{l_p}\int_{x=l_n+l_s}^{L}\frac{\partial}{\partial x}\left(D_{2p}\frac{\partial c_2}{\partial x}\right)dx = \frac{1}{l_p}\left(D_{2p}\frac{\partial c_2}{\partial x}\right)_{x=l_n+l_s}^{L} = \frac{q_{2ip}}{l_p}. \tag{46}$$

Volume averaging of the accumulation and reaction rate terms in equation (33) is as before. Finally, the volume averaged electrolyte diffusion equation in the positive electrode region is

$$l_p\varepsilon_{2p}\frac{d\langle c_2\rangle_p}{dt} = q_{2ip} + (1-t_+)a_p l_p\langle j_p\rangle. \tag{47}$$

The evolution equations for the average electrolyte concentrations in the three regions, equations (43), (45) and (47), are not independent of each other. During discharge, in the negative electrode, when an Li^+ ion gets into the electrolyte an electron gets released into the outer circuit. This electron recombines with some other Li^+ in the electrolyte within the positive electrode region, almost instantaneously, neglecting electronic transients. Thus, if a Li^+ ion is released in the negative electrode region, some other Li^+ ion gets consumed in the positive electrode region. Hence, an overall electrolyte balance holds at any time

$$l_n\varepsilon_{2n}\langle c_2\rangle_n + l_s\varepsilon_{2s}\langle c_2\rangle_s + l_p\varepsilon_{2p}\langle c_2\rangle_p = (l_n\varepsilon_{2n} + l_s\varepsilon_{2s} + l_p\varepsilon_{2p})c_{20}, \tag{48}$$

where c_{20} is the initial electrolyte concentration, as in the initial condition (37). Differentiating this equation with respect to time gives

$$l_n\varepsilon_{2n}\frac{d\langle c_2\rangle_n}{dt} + l_s\varepsilon_{2s}\frac{d\langle c_2\rangle_s}{dt} + l_p\varepsilon_{2p}\frac{d\langle c_2\rangle_p}{dt} = 0. \tag{49}$$

Adding up equations (43), (45) and (47), and using the electroneutrality condition (13), it is easily seen that (49) is satisfied.

In the volume averaged electrolyte diffusion equations (43), (45) and (47), the interfacial fluxes appear explicitly, hence they are identified as physically relevant internal variables characterizing the cell behavior. As noted earlier, these volume averaged results are exact and not approximations, even though they entail loss of concentration profile or gradient information.

3.3. Profile approximations

3.3.1. Negative electrode region

While deriving the volume averaged equation for the negative electrode region, the volume average of the diffusive flux gradient term in the electrolyte diffusion equation is given by the exact result, equation (41). To approximate the concentration profile in the negative electrode region, it is assumed that

$$\frac{\partial}{\partial x}\left(D_{2n}\frac{\partial c_2}{\partial x}\right) \approx -\frac{q_{2in}}{l_n}. \tag{50}$$

This expression is the lowest order approximation which on volume averaging will satisfy the exact result equation (41). Higher order approximations are not warranted when uniform reaction rate approximations are used for the reaction rates, as in equation (16). This approximation illustrates the basic approach of this work: approximations are always constructed such that on volume averaging they respect the exact results from volume averaged field equations. This approach ensures that errors vanish at the domain (electrode or separator regions) volume level. The uniform reaction

rate approximations, equations (16) and (17), also followed this approach, trivially though.

The profile approximation (50) is integrated once with respect to x as

$$\frac{\partial}{\partial x}\left(D_{2n}\frac{\partial c_2}{\partial x}\right) = -\frac{q_{2in}}{l_n} \Rightarrow D_{2n}\frac{\partial c_2}{\partial x} = -\frac{q_{2in}}{l_n}x + f(t), \tag{51}$$

where $f(t)$ is some arbitrary function. Applying the boundary condition at separator interface (27) gives

$$@x{=}l_n: -q_{2in} = -\frac{q_{2in}}{l_n}l_n + f(t) \Rightarrow f(t) = 0 \Rightarrow D_{2n}\frac{\partial c_2}{\partial x} = -\frac{q_{2in}}{l_n}x. \tag{52}$$

Note that equation (52) satisfies the collector end boundary condition (25).

Rearranging equation (52) and integrating once more with respect to x gives

$$\frac{\partial c_2}{\partial x} = -\frac{q_{2in}}{l_n D_{2n}}x \Rightarrow c_2(x,t) = -\frac{q_{2in}}{l_n D_{2n}}\frac{x^2}{2} + f(t), \tag{53}$$

where $f(t)$ is some arbitrary function. Applying the interfacial concentration boundary condition (26) gives

$$@x = l_n: \quad c_{2in} = -\frac{q_{2in}}{l_n D_{2n}}\frac{l_n^2}{2} + f(t). \tag{54}$$

Note that the interfacial concentration appears as a natural variable. Hence, it is also considered as a physically relevant internal variable along with the interfacial flux. Eliminating $f(t)$ between equations (53) and (54) gives

$$c_2(x,t) = c_{2in}(t) + \frac{q_{2in}(t)}{2l_n D_{2n}}\left(l_n^2 - x^2\right). \tag{55}$$

Once the interfacial concentration and flux are known, the electrolyte concentration profile is computed using equation (55). The rest of the model development focuses on deriving equations for the interfacial concentration and flux. Applying the volume averaging definition (7) for the quadratic term appearing in equation (55) gives

$$\left\langle x^2\right\rangle_n = \frac{1}{l_n}\int_{x=0}^{l_n} x^2 dx \Rightarrow \frac{1}{l_n}\frac{l_n^3}{3} = \frac{l_n^2}{3}. \tag{56}$$

Using this result and volume averaging equation (55) gives

$$\langle c_2\rangle_n = c_{2in} + \frac{q_{2in}}{2l_n D_{2n}}\frac{2}{3}l_n^2 = c_{2in} + \frac{l_n q_{2in}}{3D_{2n}}. \tag{57}$$

Differentiating this equation with respect to time gives

$$\frac{d\langle c_2\rangle_n}{dt} = \frac{dc_{2in}}{dt} + \frac{l_n}{3D_{2n}}\frac{dq_{2in}}{dt}. \tag{58}$$

Using the above expression in equation (43) gives

$$l_n\varepsilon_{2n}\frac{dc_{2in}}{dt} + \frac{l_n^2\varepsilon_{2n}}{3D_{2n}}\frac{dq_{2in}}{dt} = -q_{2in} + (1-t_+)a_n l_n\langle j_n\rangle. \tag{59}$$

Equation (59) is one equation for the two unknowns: interfacial concentration and interfacial flux in the negative electrode region. One more equation is needed for these two unknowns for closure. These variables are related to the interfacial concentration and flux in the positive electrode region, since an electrolyte balance (48) prevails.

The derivation above assumes that electrolyte diffusivity does not vary with electrolyte concentration, as per the cell design parameters listed in supplementary material S4. The derivation, however, can be extended to accommodate concentration dependent electrolyte diffusivity. For example, in the next section concentration dependent ionic conductivity is considered.

For later reference, from equation (55) the electrolyte concentration near the negative collector end is obtained as

$$c_2(x = 0, t) = c_{2in}(t) + \frac{q_{2in}(t)l_n}{2D_{2n}}. \tag{60}$$

3.3.2. Positive electrode region

The derivation is analogous to the one above, so only the salient steps are presented. From equation (46), the profile approximation is derived as

$$\frac{\partial}{\partial x}\left(D_{2p}\frac{\partial c_2}{\partial x}\right) \approx \frac{q_{2ip}}{l_p}. \tag{61}$$

This approximation is integrated with respect to x once and the boundary condition at the collector end (36) is applied to get

$$D_{2p}\frac{\partial c_2}{\partial x} = -\frac{q_{2ip}}{l_p}(L - x). \tag{62}$$

Note that this equation satisfies the interfacial flux boundary condition (35).

Integrating once again with respect to x and applying the interfacial concentration boundary condition (34) leads to

$$c_2(x,t) = c_{2ip}(t) - \frac{q_{2ip}(t)}{2l_p D_{2p}}\left[l_p^2 - (L-x)^2\right]. \tag{63}$$

Using the volume average definition (8), the volume average of the quadratic appearing in the above equation is

$$\left\langle (L-x)^2\right\rangle_p = \frac{l_p^2}{3}. \tag{64}$$

Using this result and volume averaging equation (63) gives

$$\langle c_2\rangle_p = c_{2ip} - \frac{l_p q_{2ip}}{3D_{2p}}. \tag{65}$$

Differentiating this with respect to time and using it in equation (47) gives

$$l_p\varepsilon_{2p}\frac{dc_{2ip}}{dt} - \frac{l_p^2\varepsilon_{2p}}{3D_{2p}}\frac{dq_{2ip}}{dt} = q_{2ip} + (1-t_+)a_p l_p\left\langle j_p\right\rangle. \tag{66}$$

For later reference, from equation (63) the electrolyte concentration near the positive collector end is obtained as

$$c_2(x = L, t) = c_{2ip}(t) - \frac{q_{2ip}(t)l_p}{2D_{2p}}. \tag{67}$$

3.3.3. Separator region

From equation (44) the profile approximation is derived as

$$\frac{\partial}{\partial x}\left(D_{2s}\frac{\partial c_2}{\partial x}\right) \approx \frac{q_{2in} - q_{2ip}}{l_s}. \tag{68}$$

The electrolyte diffusion equation (28) shows that the above expression is the lowest order approximation which can support an accumulation of electrolyte in the separator region. Electrolyte

accumulation or depletion in the separator is expected during high current transients. This expression is integrated once with respect to x, and the negative electrode side flux boundary condition (30) is applied to give

$$D_{2s}\frac{\partial c_2}{\partial x} = -q_{2in} + \left(\frac{q_{2in} - q_{2ip}}{l_s}\right)(x - l_n). \tag{69}$$

Note that this equation satisfies the positive electrode side flux boundary condition (32). Integrating once again with respect to x and applying the negative electrode side interfacial concentration boundary condition (29) gives

$$c_2(x,t) = c_{2in}(t) - \frac{q_{2in}(t)}{D_{2s}}(x - l_n) + \left(\frac{q_{2in}(t) - q_{2ip}(t)}{l_s D_{2s}}\right)\frac{(x - l_n)^2}{2}. \tag{70}$$

Note that the positive electrode side interfacial concentration boundary condition (31) is not yet utilized. Applying it on equation (70) gives an algebraic equation between the interfacial concentrations and fluxes

$$c_{2in} - c_{2ip} = \frac{l_s\left(q_{2in} + q_{2ip}\right)}{2D_{2s}}. \tag{71}$$

This equation can be rearranged as

$$D_{2s}\frac{c_{2in} - c_{2ip}}{l_s} = \frac{q_{2in} + q_{2ip}}{2}, \tag{72}$$

and rationalized as the relationship between average concentration gradient and the average flux, under the assumption of quadratic spatial dependence of electrolyte concentration.

Using the definition of volume averaging in the separator region (38), the volume average of linear and quadratic terms appearing in concentration profile (70) are obtained as

$$\langle (x - l_n)\rangle_s = \frac{1}{l_s}\frac{l_s^2}{2} = \frac{l_s}{2}, \quad \left\langle (x - l_n)^2 \right\rangle_s = \frac{1}{l_s}\frac{l_s^3}{3} = \frac{l_s^2}{3}. \tag{73}$$

Using these results, volume averaging equation (70) gives

$$\langle c_2\rangle_s = c_{2in} - \frac{l_s q_{2in}}{3D_{2s}} - \frac{l_s q_{2ip}}{6D_{2s}}. \tag{74}$$

Since the time derivatives of the average concentrations are not independent of each other, due to equation (49), the above equation needs not be differentiated with respect to time and used in the volume averaged diffusion equation (45) of the separator. Thus, the profile approximations in the three regions have yielded three equations (59), (66) and (71) for the four unknowns: two interfacial concentrations and two interfacial fluxes. The fourth equation is stipulated among these four unknowns by the overall electrolyte balance. Substituting the average concentrations of the three regions (57), (65) and (74) in the overall electrolyte balance (48), and rearranging gives

$$(l_n\varepsilon_{2n} + l_s\varepsilon_{2s})c_{2in} + \left(\frac{l_n^2\varepsilon_{2n}}{3D_{2n}} - \frac{l_s^2\varepsilon_{2s}}{3D_{2s}}\right)q_{2in} + l_p\varepsilon_{2p}c_{2ip} - \left(\frac{l_p^2\varepsilon_{2p}}{3D_{2p}} + \frac{l_s^2\varepsilon_{2s}}{6D_{2s}}\right)q_{2ip} = (l_n\varepsilon_{2n} + l_s\varepsilon_{2s} + l_p\varepsilon_{2p})c_{20}. \tag{75}$$

Now, with four equations for the four unknowns, the formulation is closed.

For later reference, from equation (70) the electrolyte concentration in the middle of the separator is obtained as

$$c_{2mid} \equiv c_2\left(l_n + \frac{l_s}{2}, t\right) = c_{2in} - \frac{3l_s}{8D_{2s}}q_{2in} - \frac{l_s}{8D_{2s}}q_{2ip}. \tag{76}$$

3.3.4. Reduction from a (4 × 4) system to a (2 × 2) system

Among the four equations for the four unknowns, two are ODEs (59) and (66) while two are linear algebraic equations (71) and (75). The linear algebraic equations can be solved for the interfacial concentrations in terms of the interfacial fluxes, and eventually the ODEs solved only for the interfacial fluxes. By this reduction, instead of solving 4 equations for 4 unknowns, only 2 ODEs are solved for the two interfacial fluxes.

Equation (71) is rearranged as

$$c_{2in} = c_{2ip} + \frac{l_s\left(q_{2in} + q_{2ip}\right)}{2D_{2s}}. \tag{77}$$

Substituting this expression for c_{2in} in equation (75) and rearranging gives

$$c_{2ip} = c_{20} + \alpha_{in}q_{2in} + \alpha_{ip}q_{2ip}, \tag{78}$$

where

$$\alpha_{in} = -\left(\frac{l_n l_s\varepsilon_{2n}}{2D_{2s}} + \frac{l_s^2\varepsilon_{2s}}{6D_{2s}} + \frac{l_n^2\varepsilon_{2n}}{3D_{2n}}\right)\frac{1}{(l_n\varepsilon_{2n} + l_s\varepsilon_{2s} + l_p\varepsilon_{2p})}, \tag{79}$$

and

$$\alpha_{ip} = -\left(\frac{l_n l_s\varepsilon_{2n}}{2D_{2s}} + \frac{l_s^2\varepsilon_{2s}}{3D_{2s}} - \frac{l_p^2\varepsilon_{2p}}{3D_{2p}}\right)\frac{1}{(l_n\varepsilon_{2n} + l_s\varepsilon_{2s} + l_p\varepsilon_{2p})}. \tag{80}$$

Differentiating equation (78) with respect to time gives

$$\frac{dc_{2ip}}{dt} = \alpha_{in}\frac{dq_{2in}}{dt} + \alpha_{ip}\frac{dq_{2ip}}{dt}. \tag{81}$$

Similarly differentiating equation (75) with respect to time, using equation (81) in it for the time derivative of c_{2ip} and rearranging gives

$$\frac{dc_{2in}}{dt} = \left(\alpha_{in} + \frac{l_s}{2D_{2s}}\right)\frac{dq_{2in}}{dt} + \left(\alpha_{ip} + \frac{l_s}{2D_{2s}}\right)\frac{dq_{2ip}}{dt}. \tag{82}$$

Equations (81) and (82) express interfacial concentration derivatives in terms of interfacial flux derivatives. Using these equations, interfacial concentration derivatives are eliminated from equations (59) and (66) to give

$$\left(l_n\varepsilon_{2n}\alpha_{in} + \frac{l_s l_n\varepsilon_{2n}}{2D_{2s}} + \frac{l_n^2\varepsilon_{2n}}{3D_{2n}}\right)\frac{dq_{2in}}{dt} + \left(l_n\varepsilon_{2n}\alpha_{ip} + \frac{l_n l_s\varepsilon_{2n}}{2D_{2s}}\right)\frac{dq_{2ip}}{dt} = -q_{2in} + (1 - t_+)a_n l_n\langle j_n\rangle, \tag{83}$$

and

$$l_p\varepsilon_{2p}\alpha_{in}\frac{dq_{2in}}{dt} + \left(l_p\varepsilon_{2p}\alpha_{ip} - \frac{l_p^2\varepsilon_{2p}}{3D_{2p}}\right)\frac{dq_{2ip}}{dt} = q_{2ip} + (1 - t_+)a_p l_p\left\langle j_p\right\rangle. \tag{84}$$

These are the evolution equations for the interfacial fluxes. Assuming an equilibrated initial state, these interfacial fluxes have zero initial condition. Once they are solved for, c_{2ip} is obtained using equation (78), and c_{2in} is obtained using equation (77). In the right

hand side of the original ODEs (59) and (66) only the interfacial fluxes appear and not the interfacial concentrations. Hence, it was simpler to eliminate interfacial concentrations using the algebraic equations (71) and (75), rather than trying to eliminate the interfacial fluxes.

4. Total current balance equations

4.1. Field equations

The total current at any point in the cell is the sum of solid current (Ohmic component in the solid phase), migration current (electrolyte migration due to electric potential gradient) and diffusion current (current carried by diffusive flux caused by concentration gradient). In the separator only migration and diffusion currents exist. The electrolyte potential field is continuous across the three regions; hence, like electrolyte concentration field, electrolyte potential and migration current continuities apply at the electrode–separator interfaces. At the collector ends, migration currents go to zero and solid currents equal the external current. At the electrode–separator interfaces, solid currents go to zero, so that the sum of migration and diffusion currents equals the total current. The interfacial electrolyte potential and interfacial migration currents are identified as separate variables, so that is easy to impose them in the individual regions, and maintain their equality across the interfaces.

4.1.1. Negative electrode region

$$-\sigma_{1n}\frac{\partial \Phi_1}{\partial x}-\kappa_{2n}\frac{\partial \Phi_2}{\partial x}+2\kappa_{2n}\frac{RT}{F}(1-t_+)\frac{\partial \ln c_2}{\partial x}=I, \tag{85}$$

with boundary conditions

$$-\kappa_{2n}\frac{\partial \Phi_2}{\partial x}\bigg|_{x=0}=0, \tag{86}$$

$$\Phi_2(l_n,t)=\Phi_{2in}(t), \tag{87}$$

$$\text{and } -\kappa_{2n}\frac{\partial \Phi_2}{\partial x}\bigg|_{x=l_n}=I_{2in}(t). \tag{88}$$

4.1.2. Separator region

$$-\kappa_{2s}\frac{\partial \Phi_2}{\partial x}+2\kappa_{2s}\frac{RT}{F}(1-t_+)\frac{\partial \ln c_2}{\partial x}=I, \tag{89}$$

with boundary conditions

$$\Phi_2(l_n,t)=\Phi_{2in}(t), \tag{90}$$

$$-\kappa_{2s}\frac{\partial \Phi_2}{\partial x}\bigg|_{x=l_n}=I_{2in}(t), \tag{91}$$

$$\Phi_2(l_n+l_s,t)=\Phi_{2ip}(t), \tag{92}$$

$$\text{and } -\kappa_{2s}\frac{\partial \Phi_2}{\partial x}\bigg|_{x=l_n+l_s}=I_{2ip}(t). \tag{93}$$

One needs to assume a reference potential (either for electrolyte or solid potential) somewhere within the cell. This work takes a zero reference potential at the center of the separator

$$\Phi_2\left(l_n+\frac{l_s}{2},t\right)=0. \tag{94}$$

Having an electrolyte potential reference within the separator eases out analytical integration in the reduced order model development as shown below, since solid current component is absent in the separator total current balance (89). The cell voltage is the difference in solid potential between the two collector ends. Hence, the choice of reference potential (both location and value) does not affect the cell voltage.

4.1.3. Positive electrode region

$$-\sigma_{1p}\frac{\partial \Phi_1}{\partial x}-\kappa_{2p}\frac{\partial \Phi_2}{\partial x}+2\kappa_{2p}\frac{RT}{F}(1-t_+)\frac{\partial \ln c_2}{\partial x}=I, \tag{95}$$

with boundary conditions

$$\Phi_2(l_n+l_s,t)=\Phi_{2ip}(t), \tag{96}$$

$$-\kappa_{2p}\frac{\partial \Phi_2}{\partial x}\bigg|_{x=l_n+l_s}=I_{2ip}(t), \tag{97}$$

$$\text{and } -\kappa_{2p}\frac{\partial \Phi_2}{\partial x}\bigg|_{x=L}=0. \tag{98}$$

4.2. Electrolyte potential profiles

For algebraic ease let

$$\Theta=\frac{RT}{F}(1-t_+). \tag{99}$$

4.2.1. Separator region

The electrolyte concentration profile in the separator is known from equation (70), using this profile, equation (89) can be directly integrated to get the electrolyte potential profile in the separator. Ionic conductivity is often a strong function of electrolyte concentration. In the reduced order framework, however, it is laborious to handle spatial variation of material properties. Due to the thinness of the electrode or separator regions, ionic conductivity is assumed to be a function of the volume average concentration, instead of the local concentration:

$$\kappa_{2s}(x,t)=\kappa_2[c_2(x,t)]\times\varepsilon_{2s}^{brug}\ \Rightarrow\ \kappa_{2s}(t)\approx\kappa_2[\langle c_2\rangle_s(t)]\times\varepsilon_{2s}^{brug}. \tag{100}$$

Note that the temporal variations of the ionic conductivity are accounted through average electrolyte concentration. Equation (89) is rearranged to get

$$\frac{\partial \Phi_2}{\partial x}=2\Theta\frac{\partial \ln c_2}{\partial x}-\frac{I(t)}{\kappa_{2s}(t)}. \tag{101}$$

Integrating the above equation with respect to x gives

$$\Phi_2(x,t)=2\Theta\ln c_2-\frac{I(t)}{\kappa_{2s}(t)}x+f(t), \tag{102}$$

where $f(t)$ is some arbitrary function. Applying the potential reference (94) gives

$$0 = 2\Theta \ln[c_{2\mathrm{mid}}(t)] - \frac{I(t)}{\kappa_{2\mathrm{s}}(t)}\left(l_{\mathrm{n}} + \frac{l_{\mathrm{s}}}{2}\right) + f(t), \tag{103}$$

where the mid-separator concentration is got from equation (76). Eliminating $f(t)$ between equations (102) and (103) gives

$$\Phi_2(x,t) = 2\Theta \ln\left[\frac{c_2(x,t)}{c_{2\mathrm{mid}}(t)}\right] - \frac{I(t)}{\kappa_{2\mathrm{s}}(t)}\left[x - \left(l_{\mathrm{n}} + \frac{l_{\mathrm{s}}}{2}\right)\right]. \tag{104}$$

This is an exact result, subject to the diffusion approximations in the electrolyte concentration field and the approximation in equation (100). Using the above expression the electrolyte potential at the two interfaces is identified as

$$\Phi_{2\mathrm{in}}(t) = \Phi_2(l_{\mathrm{n}},t) = 2\Theta \ln\left[\frac{c_{2\mathrm{in}}(t)}{c_{2\mathrm{mid}}(t)}\right] + \frac{I(t)l_{\mathrm{s}}}{2\kappa_{2\mathrm{s}}(t)}, \tag{105}$$

$$\text{and } \Phi_{2\mathrm{ip}}(t) = \Phi_2(l_{\mathrm{n}}+l_{\mathrm{s}},t) = 2\Theta \ln\left[\frac{c_{2\mathrm{ip}}(t)}{c_{2\mathrm{mid}}(t)}\right] - \frac{I(t)l_{\mathrm{s}}}{2\kappa_{2\mathrm{s}}(t)}. \tag{106}$$

These interfacial electrolyte potentials will be used while solving for the electrolyte potential in the electrode regions, to ensure electrolyte potential continuity.

4.2.2. Negative electrode region

As before the ionic conductivity is assumed to be a function of the average electrolyte concentration in this region

$$\kappa_{2\mathrm{n}}(t) \approx \kappa_2[\langle c_2\rangle_{\mathrm{n}}(t)] \times \varepsilon_{2\mathrm{n}}^{\mathrm{brug}}. \tag{107}$$

The solid current term appears in the total current balance for negative electrode (85). The expression for solid current is taken from equation (22), rewritten in a once integrated form to facilitate integration of the total current balance equation,

$$-\sigma_{1\mathrm{n}}\frac{\partial \Phi_1}{\partial x} = \frac{I(t)}{l_{\mathrm{n}}}(l_{\mathrm{n}} - x) = \frac{\partial}{\partial x}\left[-\frac{I(t)}{l_{\mathrm{n}}}\frac{(l_{\mathrm{n}}-x)^2}{2}\right]. \tag{108}$$

Note that the uniform reaction rate approximation is entering into electrolyte potential calculation through this solid current equation. Using equation (108) in the total current balance (85) gives

$$\frac{\partial}{\partial x}\left[-\frac{I(t)}{l_{\mathrm{n}}}\frac{(l_{\mathrm{n}}-x)^2}{2}\right] - \kappa_{2\mathrm{n}}\frac{\partial \Phi_2}{\partial x} + 2\kappa_{2\mathrm{n}}\Theta\frac{\partial \ln c_2}{\partial x} = I. \tag{109}$$

This equation can be rearranged into a total differential as

$$\frac{\partial}{\partial x}\left[-\frac{I(t)}{l_{\mathrm{n}}}\frac{(l_{\mathrm{n}}-x)^2}{2} - \kappa_{2\mathrm{n}}\Phi_2 + 2\kappa_{2\mathrm{n}}\Theta \ln c_2\right] = I. \tag{110}$$

Ionic conductivity, according to equation (107), does not have spatial dependence. Hence, equation (107) is easily put in total differential form. Integrating once with respect to x gives

$$-\frac{I(t)}{l_{\mathrm{n}}}\frac{(l_{\mathrm{n}}-x)^2}{2} - \kappa_{2\mathrm{n}}\Phi_2 + 2\kappa_{2\mathrm{n}}\Theta \ln c_2 = Ix + f(t), \tag{111}$$

where $f(t)$ is some arbitrary function. Applying the interfacial electrolyte potential boundary condition (87) gives

$$\text{At } x = l_{\mathrm{n}}: \quad -\kappa_{2\mathrm{n}}\Phi_{2\mathrm{in}} + 2\kappa_{2\mathrm{n}}\Theta \ln c_{2\mathrm{in}} = I(t)l_{\mathrm{n}} + f(t). \tag{112}$$

Eliminating $f(t)$ between equations (111) and (112) gives

$$\Phi_2(x,t) = \Phi_{2\mathrm{in}}(t) + 2\Theta \ln\left(\frac{c_2(x,t)}{c_{2\mathrm{in}}(t)}\right) + \frac{I(t)}{\kappa_{2\mathrm{n}}}(l_{\mathrm{n}}-x) - \frac{I(t)}{2\kappa_{2\mathrm{n}}l_{\mathrm{n}}}(l_{\mathrm{n}}-x)^2. \tag{113}$$

This is an exact result, subject to the diffusion approximations in the electrolyte concentration field and uniform reaction rate approximation in the solid current expression.

For later reference, from equation (113) the electrolyte potential near the negative collector end is obtained as

$$\Phi_2(x=0,t) = \Phi_{2\mathrm{in}}(t) + 2\Theta \ln\left(\frac{c_2(x=0,t)}{c_{2\mathrm{in}}(t)}\right) + \frac{I(t)l_{\mathrm{n}}}{2\kappa_{2\mathrm{n}}}. \tag{114}$$

4.2.3. Positive electrode region

The solution procedure is similar to the one above. The solid current equation (23) is rewritten as

$$-\sigma_{1\mathrm{p}}\frac{\partial \Phi_1}{\partial x} = \frac{I(t)}{l_{\mathrm{p}}}[x-(l_{\mathrm{n}}+l_{\mathrm{s}})] = \frac{\partial}{\partial x}\left\{\frac{I(t)[x-(l_{\mathrm{n}}+l_{\mathrm{s}})]^2}{l_{\mathrm{p}}\quad 2}\right\}. \tag{115}$$

This expression is substituted in the total current balance (95), written in total differential form, integrated once and the interfacial potential boundary condition (96) is applied to get

$$\Phi_2(x,t) = \Phi_{2\mathrm{ip}}(t) + 2\Theta \ln\left(\frac{c_2(x,t)}{c_{2\mathrm{ip}}(t)}\right) - \frac{I(t)}{\kappa_{2\mathrm{p}}}[x-(l_{\mathrm{n}}+l_{\mathrm{s}})] + \frac{I(t)}{\kappa_{2\mathrm{p}}l_{\mathrm{p}}}\frac{[x-(l_{\mathrm{n}}+l_{\mathrm{s}})]^2}{2}. \tag{116}$$

For later reference, from equation (116) the electrolyte potential near the positive collector end is obtained as

$$\Phi_2(x = L,t) = \Phi_{2\mathrm{ip}}(t) + 2\Theta \ln\left(\frac{c_2(x = L,t)}{c_{2\mathrm{ip}}(t)}\right) - \frac{I(t)l_{\mathrm{p}}}{2\kappa_{2\mathrm{p}}}. \tag{117}$$

With equations (104), (113) and (116) the electrolyte potential field is fully solved. The total current balances had just first order spatial derivatives. Hence, on spatial integration, electrolyte potential continuities were enough to fix their integration constants. Thus, the migration current continuities, equations (88), (91), (93) and (97) were not utilized yet. These continuities imply that the Bruggeman factors for ionic conductivity and ionic diffusivity are identical, as shown in the supplementary material S2.

5. Solid phase mass balance equations

5.1. Field equations

Active materials in the negative and positive electrodes are idealized as mono-disperse spherical particles, with radii r_{n} and r_{p} respectively. Inert lithium species travel in and out of these active material spheres. Hence, spherical diffusion equations form the solid phase mass balances. The diffusive flux on the outer surface of these spheres matches the local electrochemical reaction rate. At the center of the sphere diffusive flux is zero, by radial symmetry. The radius of an active material sphere is a measure of the solid phase diffusion resistance. The system of equations given below is identical for the two electrodes.

$$\frac{\partial c_{1k}}{\partial t} = \frac{1}{r^2}\frac{\partial}{\partial r}\left(r^2 D_{1k}\frac{\partial c_{1k}}{\partial r}\right); \quad k = \mathrm{n,p}, \tag{118}$$

$$\text{with surface boundary condition} \quad -D_{1k}\frac{\partial c_{1k}}{\partial r}\bigg|_{r=r_k} = j_k, \tag{119}$$

$$\text{symmetry boundary condition} \quad -D_{1k}\frac{\partial c_{1k}}{\partial r}\bigg|_{r=0} = 0, \tag{120}$$

$$\text{and initial condition} \quad c_{1k}(r,0) = c_{1k0}. \tag{121}$$

5.2. Volume averaged field equations

Volume averaging of a function $f(r)$ *within a sphere* is defined as follows:

$$\overline{f} = \frac{\int_{r=0}^{r_k} 4\pi r^2 f(r)\mathrm{d}r}{\frac{4}{3}\pi r_k^3} = \frac{3}{r_k^3}\int_{r=0}^{r_k} r^2 f(r)\mathrm{d}r. \tag{122}$$

Sphere volume averaging the left hand side of equation (118) shows that volume average of the time derivative is the time derivative of the volume average

$$\mathrm{LHS} = \frac{3}{r_k^3}\int_{r=0}^{r_k}\frac{\partial c_{1k}}{\partial t}r^2\,\mathrm{d}r = \frac{\partial}{\partial t}\frac{3}{r_k^3}\int_{r=0}^{r_k} r^2 c_{1k}\,\mathrm{d}r = \frac{\mathrm{d}\overline{c}_{1k}}{\mathrm{d}t}. \tag{123}$$

The right hand side of equation (118) is sphere volume averaged, using the boundary conditions (119) and (120) as

$$\begin{aligned}\mathrm{RHS} &= \overline{\frac{1}{r^2}\frac{\partial}{\partial r}\left(r^2 D_{1k}\frac{\partial c_{1k}}{\partial r}\right)} = \frac{3}{r_k^3}\int_{r=0}^{r_k}\frac{1}{r^2}\frac{\partial}{\partial r}\left(r^2 D_{1k}\frac{\partial c_{1k}}{\partial r}\right)r^2\,\mathrm{d}r \\ &= \frac{3}{r_k^3}\left(r^2 D_{1k}\frac{\partial c_{1k}}{\partial r}\right)_{r=0}^{r_k} = -\frac{3j_k}{r_k}.\end{aligned} \tag{124}$$

Thus the sphere volume averaged solid state diffusion equation is

$$\frac{\mathrm{d}\overline{c}_{1k}}{\mathrm{d}t} = -\frac{3j_k}{r_k}. \tag{125}$$

From the original initial condition (121), the initial condition for the above ODE is obtained as

$$\overline{c}_{1k0} = c_{1ko}. \tag{126}$$

The reaction rate and the sphere average concentration in the above equation are functions of x, in general. Volume averaging across the electrode volume, using definitions (7) or (8), gives the electrode volume averaged solid state diffusion equation

$$\frac{\mathrm{d}\langle\overline{c}_{1k}\rangle}{\mathrm{d}t} = -\frac{3\langle j_k\rangle}{r_k}. \tag{127}$$

An observation regarding uniform reaction rate approximation, though it is not used in this subsection: Under uniform reaction rate approximation, the concentration fields in all the spheres within an electrode are identical; hence spherical volume average concentration is identical to electrode volume average concentration. Hence, under this approximation, equations (125) and (127) are identical.

During discharge, in the negative electrode, when a neutral solid phase Li is released into the electrolyte as a Li^+ ion and an electron is released into the outer circuit. This electron recombines with some other Li^+ in electrolyte within the positive electrode region (almost instantaneously, neglecting electronic transients), and forms a solid phase Li. Thus, if a solid phase Li decreases in the negative electrode, a solid phase Li gets formed at the positive electrode. Thus, an overall solid phase lithium balance holds at any time

$$l_\mathrm{n}\varepsilon_{1\mathrm{n}}\langle\overline{c}_{1\mathrm{n}}\rangle + l_\mathrm{p}\varepsilon_{1\mathrm{p}}\langle\overline{c}_{1\mathrm{p}}\rangle = l_\mathrm{n}\varepsilon_{1\mathrm{n}}c_{1\mathrm{n}0} + l_\mathrm{p}\varepsilon_{1\mathrm{p}}c_{1\mathrm{p}0} = \text{Constant}. \tag{128}$$

Differentiating the above equation with respect to time gives

$$l_\mathrm{n}\varepsilon_{1\mathrm{n}}\frac{\mathrm{d}\langle\overline{c}_{1\mathrm{n}}\rangle}{\mathrm{d}t} + l_\mathrm{p}\varepsilon_{1\mathrm{p}}\frac{\mathrm{d}\langle\overline{c}_{1\mathrm{p}}\rangle}{\mathrm{d}t} = 0. \tag{129}$$

This equation shows that the rates of change of average solid phase lithium concentration in the two electrodes are not independent of each other. For example, if the average solid phase concentration in the negative electrode is known, that in the positive electrode is computed from equation (128) as

$$\langle\overline{c}_{1\mathrm{p}}\rangle = c_{1\mathrm{p}0} + \frac{l_\mathrm{n}\varepsilon_{1\mathrm{n}}}{l_\mathrm{p}\varepsilon_{1\mathrm{p}}}(c_{1\mathrm{n}0} - \langle\overline{c}_{1\mathrm{n}}\rangle). \tag{130}$$

Using equation (127) in equation (129) gives

$$l_\mathrm{n}\varepsilon_{1\mathrm{n}}\left(-\frac{3\langle j_\mathrm{n}\rangle}{r_\mathrm{n}}\right) + l_\mathrm{p}\varepsilon_{1\mathrm{p}}\left(-\frac{3\langle j_\mathrm{p}\rangle}{r_\mathrm{p}}\right) = 0. \tag{131}$$

The specific surface areas of the active material spheres are

$$a_k = \frac{3\varepsilon_{1k}}{r_k}. \tag{132}$$

Using these definitions in equation (131) recovers the electro-neutrality condition (13) derived in Section 2. Only electrons move in and out of a sealed lithium cell. Hence, an overall lithium balance is obviously maintained. Due to electro-neutrality at any time the total amounts of solid phase Li and electrolyte phase Li^+ ions are individually constant. Hence, there are separate Li balances for the solid and electrolyte phases, equations (128) and (48) respectively. As noted earlier, these volume averaged results are exact, even though they entail loss of concentration profile or gradient information.

5.3. Profile approximations

The parabolic and quartic profile approximations for the solid state diffusion in a lithium cell are reported in Ref. [10], wherein it is shown that high current scenarios warrant a quartic approximation. For the sake of completeness, consistent style (volume averaging based) and notation, the quartic approximation is reworked below. The parabolic approximation derivation is given in the supplementary material S3.

For the lowest order volume average respecting parabolic approximation, the profile approximation was derived from Equation (124) as

$$\frac{1}{r^2}\frac{\partial}{\partial r}\left(r^2 D_{1k}\frac{\partial c_{1k}}{\partial r}\right) \approx -\frac{3j_k}{r_k}. \tag{133}$$

The right hand side of the above equation is independent of the radial coordinate; it is dependent only on time through the reaction rate. For a higher order approximation, the gradient of diffusive flux is assumed to be parabolic in the radial coordinate

$$\frac{1}{r^2}\frac{\partial}{\partial r}\left(r^2 D_{1k}\frac{\partial c_{1k}}{\partial r}\right) = G(t) + H(t)\frac{r^2}{r_k^2}. \tag{134}$$

From the sphere volume average definition (122), the volume average of r^2 is obtained as

$$\overline{r^2} = \frac{3}{r_k^3}\int_{r=0}^{r_k} r^2 r^2\,\mathrm{d}r = \frac{3}{r_k^3}\frac{r_k^5}{5} = \frac{3}{5}r_k^2. \tag{135}$$

Sphere volume averaging equation (134) using the above result gives

$$\overline{\frac{1}{r^2}\frac{\partial}{\partial r}\left(r^2 D_{1k}\frac{\partial c_{1k}}{\partial r}\right)} = G + \frac{3}{5}H = -\frac{3j_k}{r_k}. \tag{136}$$

This gives one equation for the two unknowns G and H. Rearranging equation (134) and integrating once with respect to r gives

$$\begin{aligned}\frac{\partial}{\partial r}\left(r^2 D_{1k}\frac{\partial c_{1k}}{\partial r}\right) &= Gr^2 + H\frac{r^4}{r_k^2} \Rightarrow r^2 D_{1k}\frac{\partial c_{1k}}{\partial r}\\ &= G\frac{r^3}{3} + H\frac{r^5}{5r_k^2} + f(t),\end{aligned} \tag{137}$$

where $f(t)$ is some arbitrary function. Using the symmetry boundary condition (120) it is easily seen that $f(t)$ is zero. Hence,

$$r^2 D_{1k}\frac{\partial c_{1k}}{\partial r} = G\frac{r^3}{3} + H\frac{r^5}{5r_k^2}. \tag{138}$$

It is easily seen that applying the surface flux boundary condition (119) reduces the above equation to (136). Hence, the surface flux boundary condition does not generate another equation for the two unknowns. Equation (138) is rearranged as

$$\frac{\partial c_{1k}}{\partial r} = \frac{G}{3D_{1k}}r + \frac{H}{5D_{1k}r_k^2}r^3. \tag{139}$$

The average radial gradient

$$\bar{c}_{1kr} \equiv \overline{\frac{\partial c_{1k}}{\partial r}}, \tag{140}$$

is introduced as a physically relevant variable; an evolution equation for it will be derived by the end of this subsection. For sphere volume averaging the linear and cubic terms in the right hand side of (139) the following results are needed:

$$\bar{r} = \frac{3}{r_k^3}\int_{r=0}^{r_k} r r^2\,\mathrm{d}r = \frac{3}{r_k^3}\frac{r_k^4}{4} = \frac{3}{4}r_k;\ \overline{r^3} = \frac{3}{r_k^3}\int_{r=0}^{r_k} r^3 r^2\,\mathrm{d}r = \frac{3}{r_k^3}\frac{r_k^6}{6} = \frac{1}{2}r_k^3. \tag{141}$$

Using equations (140) and (141), sphere volume averaging equation (139) and simplifying gives

$$\frac{4D_{1k}}{r_k}\bar{c}_{1kr} = G + \frac{2}{5}H. \tag{142}$$

This is a second equation for the two unknowns G and H. Equations (136) and (142) are solved simultaneously to get explicit expressions for G and H as

$$G = \frac{6}{r_k}j_k + \frac{12D_{1k}}{r_k}\bar{c}_{1kr};\quad H = -\frac{15}{r_k}j_k - \frac{20D_{1k}}{r_k}\bar{c}_{1kr}. \tag{143}$$

Integrating equation (139) once more with respect to r gives

$$c_{1k} = \frac{G}{6D_{1k}}r^2 + \frac{H}{20D_{1k}r_k^2}r^4 + f(t), \tag{144}$$

where $f(t)$ is some arbitrary function. Applying the surface concentration condition to the above equation gives

$$@r = r_k:\quad c_{sk} = \frac{G}{6D_{1k}}r_k^2 + \frac{H}{20D_{1k}r_k^2}r_k^4 + f(t). \tag{145}$$

Eliminating $f(t)$ between equations (144) and (145) gives the quartic concentration profile

$$c_{1k} = c_{sk} - \frac{G}{6D_{1k}}\left(r_k^2 - r^2\right) - \frac{H}{20D_{1k}r_k^2}\left(r_k^4 - r^4\right). \tag{146}$$

For sphere volume averaging the right hand side, equation (146) and the following result are needed:

$$\overline{r^4} = \frac{3}{r_k^3}\int_{r=0}^{r_k} r^4 r^2\,\mathrm{d}r = \frac{3}{r_k^3}\frac{r_k^7}{7} = \frac{3}{7}r_k^4. \tag{147}$$

Sphere volume averaging equation (146) and rearranging gives

$$c_{sk} = \bar{c}_{1k} + \frac{r_k^2}{15D_{1k}}G + \frac{r_k^2}{35D_{1k}}H. \tag{148}$$

Substituting the expression (143) for G and H in the above equation and simplifying gives

$$c_{sk} = \bar{c}_{1k} - \frac{r_k}{35D_{1k}}j_k + \frac{8r_k}{35}\bar{c}_{1kr}. \tag{149}$$

Under uniform reaction rate approximation, $j_k(x,t) \approx \langle j_K\rangle(t)$ is known. The spherical average concentrations are obtained by solving the sphere volume averaged solid diffusion equation (125). The rest of the subsection derives an evolution equation for the spherical average radial gradient $\bar{c}_{1kr}$. Once it is identified, equation (149) is used to feed surface concentrations to the Butler–Volmer kinetics, as shown in the next section.

Differentiating the solid state diffusion equation (118) with respect to r and using the equality of mixed derivatives gives

$$\frac{\partial}{\partial r}\left(\frac{\partial c_{1k}}{\partial t}\right) = \frac{\partial}{\partial t}\left(\frac{\partial c_{1k}}{\partial r}\right) = \frac{\partial}{\partial r}\left[\frac{1}{r^2}\frac{\partial}{\partial r}\left(r^2 D_{1k}\frac{\partial c_{1k}}{\partial r}\right)\right]. \tag{150}$$

Using the profile approximation (134) for the radial diffusive flux in the right hand side gives

$$\frac{\partial}{\partial t}\left(\frac{\partial c_{1k}}{\partial r}\right) = H\frac{2r}{r_k^2}. \tag{151}$$

Sphere volume averaging the above equation, using equation (141) for the averaging of the linear term on the right hand side, and simplifying gives

$$\frac{d\bar{c}_{1kr}}{dt} = \frac{3}{2}\frac{H}{r_k}. \quad (152)$$

Substituting for H from equation (143) and simplifying gives the evolution equations for the average radial gradients as

$$\frac{d\bar{c}_{1kr}}{dt} + \frac{30D_{1k}}{r_k^2}\bar{c}_{1kr} = -\frac{45}{2r_k^2}j_k. \quad (153)$$

These ODEs for the average radial gradient are solved with the initial conditions

$$\bar{c}_{1kr}(r,0) = 0, \quad (154)$$

when the initial states are in equilibrium, with no concentration gradients.

6. Butler–Volmer kinetics

Butler–Volmer kinetics for the electrochemical reactions occurring on the surface of the active material spheres in the electrodes are

$$j_k = 2j_{k0}\sinh\left[\frac{F}{2RT}(\Phi_1 - \Phi_2 - U_k)\right]; \quad k = \mathrm{n,p}, \quad (155)$$

where

$$j_{k0} = k_k(c_{sk\max} - c_{sk})^{0.5}c_{sk}^{0.5}c_2^{0.5}, \quad (156)$$

and U_k are the electrode open circuit potentials.

Inverting equation (155) and rearranging gives

$$\Phi_1 = U_k + \Phi_2 + \frac{2RT}{F}\sinh^{-1}\left(\frac{j_k}{2j_{k0}}\right). \quad (157)$$

This equation is used to find the solid potential at any point within the electrodes, with the following inputs from the earlier sections:

(1) The reaction rate j_k is obtained using the uniform reaction rate approximation equations (16) or (17).
(2) The electrolyte concentration c_2, appearing in j_{k0}, is obtained from equation (55) or (63).
(3) The electrolyte potential Φ_2 is obtained from equation (113) or (116).
(4) The solid phase concentration c_{sk}, appearing in j_{k0}, is obtained from equation (148) for the quartic approximation.

The cell voltage is the solid potential difference between the positive and negative collector ends i.e.

$$V = \Phi_1(x = L) - \Phi_1(x = 0). \quad (158)$$

Since the reduced order model derivation is spread out across various sections, and the computational order is different from the derivation order, the model results are collated in the next section as a ready to use algorithm.

7. Reduced order model with uniform reaction rate approximation – algorithm

In the reduced order model framework, with a *consistent* reaction rate approximation, the electrolyte and the solid phase fields are solved in a particular order as shown in Fig. 2. In the electrolyte phase, using the reaction rate the electrolyte concentration field is solved first, which then enables the solution of the electrolyte potential field. In the solid phase, using the reaction rate the solid phase concentration field is solved. All the above fields provide input for the Butler–Volmer kinetics to solve for the solid potential field. This computational methodology is used for both the electrodes. Eventually the cell voltage is computed as the solid potential difference between the two collector ends.

For the lowest order reduced order model derived here, the reaction rates in the electrodes are assumed to be the electrode volume average reaction rates. The salient results of this model are presented below, in a sequential algorithmic order. This reduced order model predicts not just the cell voltage, but also the profiles of all the internal variables, subject to the uniform reaction rate and profile based approximations. The cell voltage and predictions from the reduced order model are compared with the detailed electrochemical model results in the next section.

7.1. Reaction rates and solid current profiles in the electrodes

External current fixes the average reaction rate in the electrodes, at any time. Under the uniform reaction rate approximation, all points within an electrode experience the same rate. The uniform reaction rates in the negative and positive electrodes are given by equations (16) and (17), respectively. Uniform reaction rate approximation implies that solid current profiles are linear. The linear current profiles in the negative and positive electrodes are given by equations (22) and (23), respectively. These internal profiles are not required for cell voltage computation.

7.2. Electrolyte concentration field in the electrode and separator regions

The electrolyte concentration field is expressed in terms of the electrode–separator interfacial concentrations and fluxes. The interfacial fluxes are obtained by solving the two coupled ODEs, equations (83) and (84), with zero initial condition for the interfacial fluxes for an equilibrated initial state. The parameters α_{in} and α_{ip} appearing in these two ODEs are obtained from equations (79) and (80), respectively. The interfacial concentrations are computed from the interfacial fluxes using equations (77) and (78). For computing the cell voltage the electrolyte concentrations at the collector ends and the middle of the separator are needed, they are obtained from equations (60), (67) and (76). The electrolyte

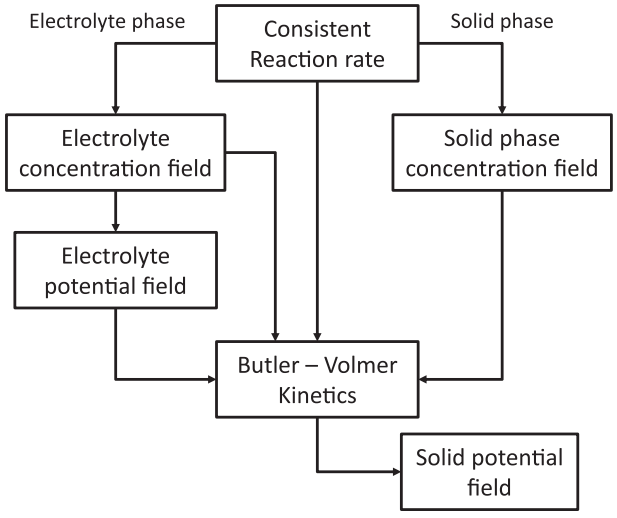

Fig. 2. Reduced order model computational methodology for an electrode.

concentration profiles in the three regions are computed using equations (55), (63) and (70). These internal profiles are not required for cell voltage computation.

7.3. Electrolyte potential field in the electrode and separator regions

The electrolyte potential field is expressed in terms of the electrode–separator interfacial potentials. In this work zero reference potential is set in the middle of the separator. These interfacial electrolyte potentials are computed from equations (105) and (106). Note that these equations use the interfacial and mid-separator electrolyte concentrations computed in the earlier subsection. The electrolyte potential at the collector ends are computed using these interfacial electrolyte potentials using equations (114) and (117). The electrolyte potential profiles in the three regions are computed using equations (104), (113) and (116). These internal profiles are not required for cell voltage computation.

7.4. Solid phase concentration field

Quartic profile approximation expresses the concentration profile within an active material sphere in terms of the average concentration and the average radial gradient. Under the uniform reaction rate approximation, all the spheres in an electrode have identical concentration field at all times (since initial concentration and reaction rates are identical). For the negative electrode the following two coupled ODEs, equations (125) and (153) are solved with initial conditions (126) and (154). The surface concentration of the negative electrode spheres is given by equation (149).

Instead of solving an ODE for the average solid phase Li concentration in the positive electrode, it is computed from the solid phase lithium balance using equation (130). The electrode volume average concentration is identical to the spherical volume average concentration under uniform reaction rate approximation. For the average radial concentration gradient in the positive electrode sphere, the ODE (153) is solved with the initial condition (154). The surface concentration of the positive electrode spheres is given by equation (149).

The concentration profiles inside the active material spheres are computed in terms of surface concentration, average radial gradient, and reaction rate using equations (143) and (146). These internal profiles are not required for cell voltage computation.

7.5. Butler–Volmer kinetics

In this reduced order framework, as shown in Fig. 2, reaction rates, electrolyte concentrations, electrolyte potentials and solid phase concentrations feed into Butler–Volmer kinetics, which is then analytically inverted to compute the solid potential. The reaction rate pre-factor in the negative electrode is computed using equation (156). The electrolyte concentration and solid phase surface concentrations therein are obtained from the earlier subsections. The solid potential in the two electrodes are computed using equation (157). The electrolyte potential and the reaction rate used therein are obtained from the earlier subsections. For cell voltage computation, equation (157) is evaluated at the two collector ends: $x = 0$ and $x = L$. Eventually, the cell voltage is computed as the difference in solid potential at the end of the two collectors as in equation (158).

7.6. Model reduction summary

The detailed electrochemical isothermal model solves 10 coupled partial differential equations: two solid phase current balance equations (1) and (4), three electrolyte diffusion equations (24), (28) and (33), three total current balance equations (85), (89) and (95), and two solid phase diffusion equations – equation (118) applied for negative and positive electrode spheres individually. The isothermal reduced order model reported herein solves 5 linear differential equations: two for the interfacial fluxes equations (83) and (84), one for the average concentration in the negative electrode sphere equation (125), and two for the average concentration gradients in the negative and positive electrode spheres equation (153). Thus instead of solving 10 coupled PDEs, this ROM solves only 5 linear ODEs. This complexity reduction was achieved using uniform reaction rate and profile approximations.

This reduced order model is structured such that nonlinearities are confined to the final algebraic evaluations (Computation of electrolyte potential by analytical integration, e.g. Equation (113) and inversion of Butler–Volmer kinetics, e.g. Equation (157)) and the five ODEs being solved are linear. The ideal model reduction that can be achieved is abstracted in Fig. 3. A dynamical system of engineering interest is often described by nonlinear PDEs. Through suitable approximations one can reduce the dynamical information into a system of linear ODEs and relegate the nonlinearities to algebraic expressions, as in this work. The nonlinearity of the problem, once relegated to algebraic expressions, is not bothersome because linear coupled ODEs can be solved without iteration. Such a time marching algorithm with minimal computational complexity is needed for on-board control applications.

7.7. Voltage transients during rest

Uniform reaction rate approximation equates the local reaction rate everywhere within an electrode to the volume average reaction rate, and the volume average reaction rate is proportional to the external current at any time. Hence, if external current is cut off, under this approximation, reaction rate goes to zero instantaneously. One of the causes for the voltage transients during rest is the relaxation of concentration gradients within active material spheres. This phenomenon is captured by the quartic approximation for solid diffusion presented above. Since the local reaction rate goes to zero instantaneously under uniform reaction rate approximation, the average concentration within the active material spheres remains frozen according to the equation (125). The surface concentration in an active material sphere given by equation (149), however, can change as the average radial gradient decreases during rest. Once the surface concentration feeding into Butler–Volmer kinetics changes, solid potential changes, leading to voltage transients. The right hand side of equation (149) shows the two pathways by which surface concentration relaxes during rest: one by reaction rate and another by radial concentration gradient. Most of the voltage relaxation during rest is expected to arise from the relaxation of

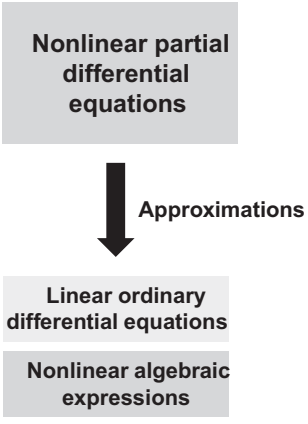

Fig. 3. Ideal model reduction methodology.

concentration gradients; this pathway is captured by the current model. The spatially varying reaction rate can also contribute to voltage relaxation during rest; this pathway is not captured by the current model.

8. Comparison of reduced order model predictions with the detailed electro-chemical model results

In this section cell voltage predictions from the reduced order model with uniform reaction rate approximation are compared with those from the detailed electrochemical model (default model in Comsol Multiphysics®) for a typical commercial cell for constant current and pulse protocols. The cell design parameters used in the Comsol® model are presented in the supplementary material S4.

8.1. Constant current protocols

The cell voltage predictions for 1C constant current discharge are shown in Fig. 4, the absolute and percentage errors in the ROM prediction in Figs. 5 and 6, respectively. At 1C constant current discharge ROM gives a maximum error of about 9 mV and a maximum percentage error of about 0.27% as shown by these figures. The corresponding figures for 7C constant current discharge are Figs. 7–9, which show that the current ROM gives a maximum error of about 80 mV and a maximum percentage error of about 3.2%. It is interesting to note that with uniform reaction rate approximation and the leading order quadratic approximation for the electrolyte concentrations in the three regions, the cell voltage prediction has less than 3.2% error, even at high current discharge.

8.2. Pulse protocols

A typical low current pulse protocol is shown in Fig. 10. It has 2000 s of 1C discharge, followed by 300 s of rest, 2000 s of 1C charge, and rest till 8000 s. The cell voltage predictions are compared in Fig. 11, and the percentage error in ROM prediction is shown in Fig. 12. The latter figure shows that the maximum percentage error is about 0.2%. The maximum absolute error (figure not shown) is about 10 mV, occurring during constant current periods.

A typical high current pulse protocol is shown in Fig. 13. It has 10 s of 7C discharge followed by 40 s of rest, 10 s of 7C charge, and 60 s of rest. The cell voltage predictions are compared in Fig. 14, and the percentage error in ROM prediction is shown in Fig. 15. The maximum percentage error is about 2% as shown in the latter figure. The maximum absolute error (figure not shown) is about 80 mV, occurring during constant current periods.

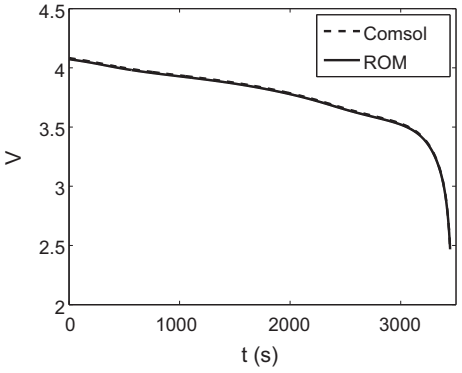

Fig. 4. Cell voltage predictions from the detailed electrochemical model (Comsol®) and the reduced order model (ROM) at 1C constant current discharge.

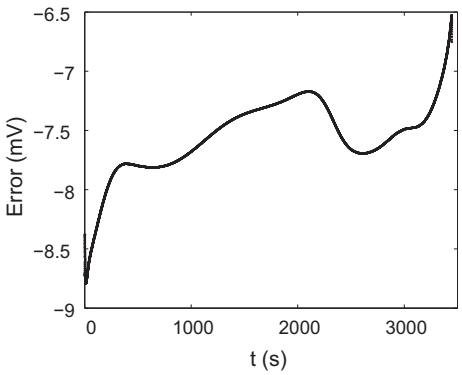

Fig. 5. Absolute error in the cell voltage predicted by the reduced order model at 1C constant current discharge.

It is interesting to note that the errors in the cell voltage predictions in both these pulse protocols during the rest periods are negligible (in Fig. 12 period 2000–2300 s, in Fig. 15 periods 10–50 s and 60–120 s). These results show that the voltage transients at the beginning of the rest periods are well captured by ROM at the current levels of approximation.

9. Summary

The detailed electrochemical model for a single cell comprises of 10 coupled partial differential equations (PDEs), for an isothermal operation. It is computationally intensive to use this model for battery packs, battery management system algorithms, calendar or cycle life predictions, detailed parameter estimation, inclusion of complex degradation mechanisms etc. This work describes a reduced order model (ROM) framework, which reduces the detailed model PDEs, to a manageable set of ordinary differential equations (ODEs), which can be used for the above applications.

Volume averaging PDEs yield ODEs. Hence volume averaging is the basic method used for model reduction. The gradient or profile information lost on volume averaging is recovered through profile based approximations. The electrolyte concentration profiles are expressed in terms of electrode–separator interfacial concentrations and fluxes. From the detailed model, equations are derived for these physically relevant internal variables.

In the ROM framework, with a *consistent* reaction rate approximation, the electrolyte and the solid phase fields are solved as follows: In the electrolyte phase, using the reaction rate the electrolyte concentration field is solved first, which then enables the solution of the electrolyte potential field. In the solid phase, using the reaction rate the solid phase concentration field is solved. All the

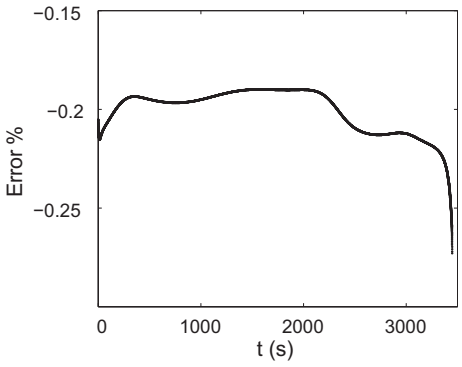

Fig. 6. Percentage error in the cell voltage predicted by the reduced order model at 1C constant current discharge.

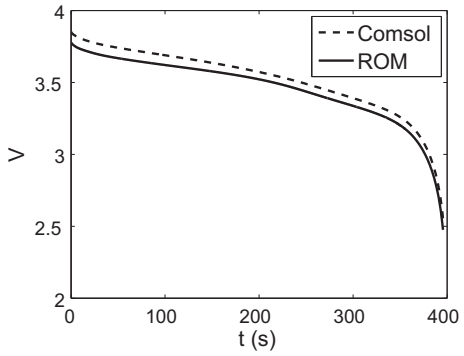

Fig. 7. Cell voltage predictions from the detailed electrochemical model (Comsol®) and the reduced order model (ROM) at 7C constant current discharge.

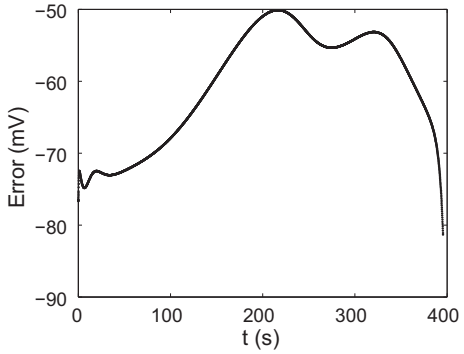

Fig. 8. Absolute error in the cell voltage predicted by the reduced order model at 7C constant current discharge.

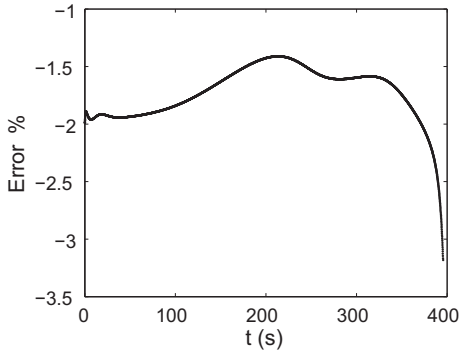

Fig. 9. Percentage error in the cell voltage predicted by the reduced order model at 7C constant current discharge.

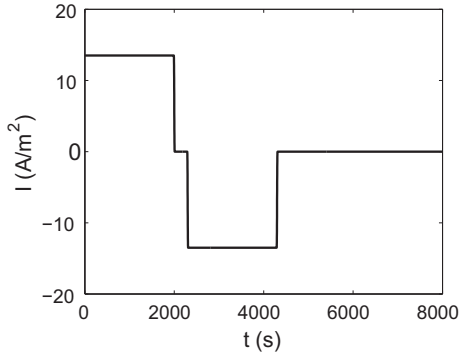

Fig. 10. A low current pulse protocol used to compare the reduced order model and the detailed electrochemical model.

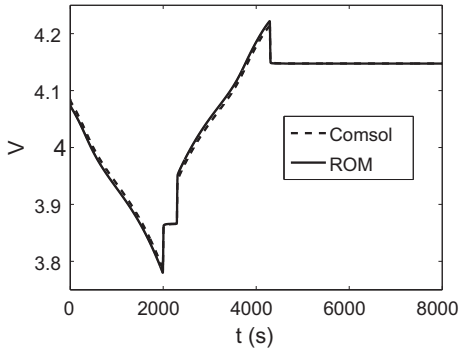

Fig. 11. Cell voltage predictions from the detailed electrochemical model (Comsol®) and the reduced order model (ROM) for the low current pulse protocol in Fig. 10.

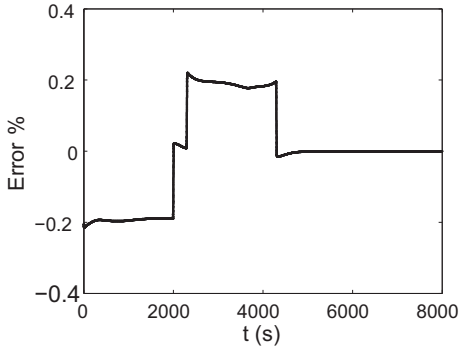

Fig. 12. Percentage error in the cell voltage predicted by the reduced order model for the low current pulse protocol in Fig. 10.

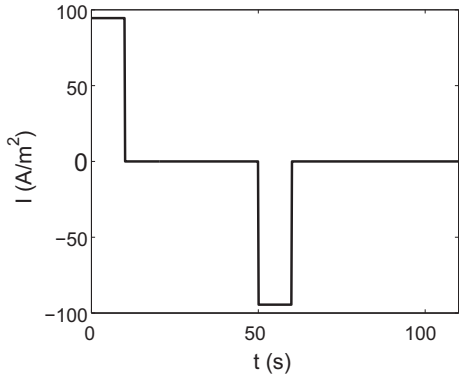

Fig. 13. A typical high current pulse protocol used to compare the reduced order model and the detailed electrochemical model.

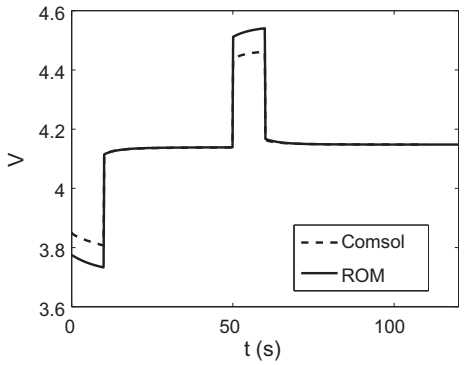

Fig. 14. Cell voltage predictions from the detailed electrochemical model (Comsol®) and the reduced order model (ROM) for the high current pulse protocol in Fig. 13.

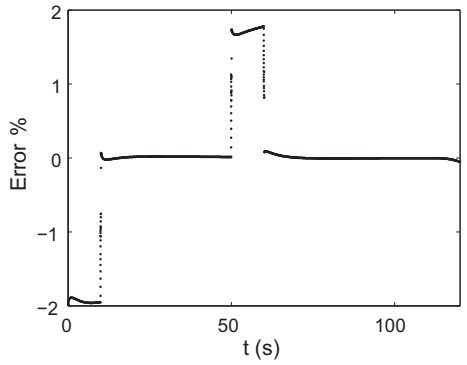

Fig. 15. Percentage error in the cell voltage predicted by the reduced order model for the high current pulse protocol in Fig. 13.

above fields provide input for the Butler–Volmer kinetics to solve for the solid potential field. This computational methodology is used for both the electrodes. Eventually the cell voltage is computed as the solid potential difference between the two collector ends.

For the lowest order ROM, a uniform reaction rate, quadratic electrolyte concentrations and quartic solid phase concentrations are assumed. In this ROM only 5 linear ODEs are solved, and the rest are nonlinear algebraic expressions. When compared with the detailed electrochemical model, this ROM gives a maximum error of about 0.27% during 1C discharge and about 3.2% during 7C discharge, for a typical commercial cell.

Acknowledgments

The author would like to thank Mark Verbrugge, Mark Mathias, Garima Bhatia, Kamakshi Jagannathan, Krishnan Hariharan, Wenbin Gu and Puneet Sinha for their constructive comments/inputs during the course of model development.

Appendix A. Supplementary material

Supplementary material associated with this article can be found, in the online version, at http://dx.doi.org/10.1016/j.jpowsour.2012.09.013.

References

[1] M. Doyle, J. Newman, J. Electrochem. Soc. 143 (1996) 1890–1903.
[2] V.R. Subramanian, V. Boovaragavan, V.D. Diwakar, Electrochem. Solid-State Lett. 10 (2007) A255–A260.
[3] M. Guo, G. Sikha, R.E. White, J. Electrochem. Soc. 158 (2011) A122–A132.
[4] N. Curle, The Laminar Boundary Layer Equations, Oxford University Press, London, 1962.
[5] E. Glueckauf, Trans. Faraday Soc. 51 (1955) 1540–1551.
[6] C.H. Liaw, J.S.P. Wang, R.A. Greenkorn, K.C. Chao, AIChE J. 25 (1979) 376–381.
[7] D.D. Do, R.G. Rice, AIChE J. 32 (1986) 149–154.
[8] T. Tomida, B.J. McCoy, AIChE J. 33 (1987) 1908–1911.
[9] M. Goto, J.M. Smith, B.J. McCoy, Chem. Eng. Sci. 45 (1990) 443–448.
[10] V.R. Subramanian, V.D. Diwakar, D. Tapriyal, J. Electrochem. Soc. 152 (2005) A2002–A2008.

Notation

Constants and variables

A: electrode cross sectional area, m^2
$a_k = 3\varepsilon_{1k}/r_k$*:* specific surface area of active materials in n and p electrodes, m^{-1}
brug: Bruggeman factor, used to calculate effective porous media properties, dimensionless
c_1, c_2*:* solid phase concentration in active material spheres and electrolyte concentration, mol m^{-3}
c_{sk}, $c_{sk\ max}$*:* surface solid phase concentrations, and their maximum value, mol m^{-3}
c_{2ik}, q_{2ik}*:* interfacial electrolyte concentrations and fluxes, mol m^{-3}, mol m^{-2} s^{-1}
D_2*:* electrolyte diffusivity (material property), m^2 s^{-1}
$D_{2k} = D_2 \times \varepsilon_{2k}^{brug}$*,:* effective electrolyte diffusivity in the porous k = n,s,p domains
D_{1k}*:* solid diffusivity of k = n,p electrode material spheres, m^2 s^{-1}
F: Faraday's constant, 96,487C mol^{-1}
I: external current density, A m^{-2}
j_k*:* local surface reaction rate in k = n, p electrodes, mol m^{-2} s^{-1}
$j_{k0} = k_k(c_{skmax} - c_{sk})^{0.5}c_{sk}^{0.5}c_2^{0.5}$*:* over-potential independent rate pre-factor, mol m^{-2} s^{-1}
k_k*:* surface reaction rate constant in k = n, p electrodes, (mol m^{-2} s^{-1})(mol m^{-3})$^{-1.5}$
l_n, l_s, l_p*:* thickness of negative electrode, separator and positive electrode, m. $L = l_n + l_s + l_p$ is total cell thickness
R: gas constant, 8.314 J mol^{-1} K^{-1}
r_n, r_p*:* Radii of active material spheres in the negative and positive electrodes, m
$SOC_k = c_{sk}/c_{skmax}$*:* state of charge of k = n, p electrodes, dimensionless
T: temperature, 298 K in this work
t_+*:* electrolyte transference number, dimensionless
U_k*:* open circuit voltage of k = n, p electrodes, V
ε_{1k}, ε_{2k}, ε_{fk}*:* volume fractions of active material, electrolyte and filler in electrode or separator domains, dimensionless. $\varepsilon_{1k} + \varepsilon_{2k} + \varepsilon_{fk} = 1$. Separator has no active material. Hence $\varepsilon_{1s} = 0$
κ_2*:* electrolyte conductivity (material property), S m^{-1}
$\kappa_{2k} = \kappa_2 \times \varepsilon_{2k}^{brug}$*:* effective electrolyte conductivity in porous k = n,s,p domains
σ_k*:* electrical conductivity of k = n,p electrode materials (material property), S m^{-1}
$\sigma_{1k} = \sigma_k \times \varepsilon_{1k}^{brug}$*:* effective electrical conductivity in the porous k = n,p domains, S m^{-1}
Φ_1, Φ_2*:* solid and liquid potential, V

Operators and subscripts

$\langle\cdot\rangle$*:* volume average, defined in the three domains, n,s,p
$\bar{\cdot}$*:* volume average within an active material sphere in n or p electrode
0: initial condition
1, 2, f: solid active material, liquid electrolyte phases and solid fillers (including additives)
in: separator interface of the negative electrode
ip: separator interface of the positive electrode
k = *n,s,p:* negative electrode, separator, and positive electrode
r: radial gradient